A Multiomics Approach for Investigating Nitrogen Metabolism in Pancreatic Cancer

Peter Sajjakulnukit, Kira Holton, Tianrui Ma, Zhengxu Tang, Michael Akpabey

19APR2024

ABSTRACT

Pancreatic ductal adenocarcinoma (PDAC) is the most common form of pancreatic cancer and one of the deadliest types of cancer with a five-year survival rate of 12%. Mutations in KRAS are present in over 90% of patients, resulting in upregulation of a non-canonical glutamine metabolic pathway. Glutamine is a major bioenergetic fuel for proliferating cells, as it generates nitrogen used for the biosynthesis of numerous essential molecules. PDAC is reliant on GOT1, a transaminase which enables the non-canonical glutamine metabolism and PDAC cell growth. However, the products from the nitrogen flux generated by GOT1 remain uncharacterized. To identify these uncharacterized targets of GOT1 glutamine metabolism, we utilized 15N2-Glutamine. We examined the effect of GOT1 knockdown on nitrogen metabolism in PDAC using untargeted and targeted metabolomics. RNA-seq data from the same GOT1 knockdown cell line was analyzed to study changes in the transcriptome, with a focus on genes involved in metabolic pathways. Integration of our metabolomic and transcriptomic data resulted in the identification of several differentially regulated metabolic pathways with nitrogen-containing compounds. Purine and pyrimidine metabolism were downregulated, suggesting deficiencies in DNA and/or RNA synthesis and thus cellular proliferation. Sphingolipid metabolism and arginine biosynthesis pathways displayed unique up- and down-regulation of distinct members, implying impacts on cellular signaling and potentially the urea cycle. Ultimately, we generated a starting point for further investigation of the nitrogen-driven metabolic signature in PDAC upon GOT1 knockdown.

INTRODUCTION

Pancreatic cancer is the fourth leading cause of all cancer deaths, with a deadly five-year survival rate of only 12%.[1] Pancreatic ductal adenocarcinoma (PDAC) is the most common form of pancreatic cancer, comprising approximately 95% of all cases.[2] It is predominantly fibrotic, with >90% of the tumor mass consisting of non-tumor related cells, and is incredibly dense, with interstitial pressures up to 10-fold higher than other organs. As PDAC is avascular, the tumor cells have limited access to oxygen and essential nutrients and undergo extensive metabolic reprogramming.[3] Furthermore, over 90% of PDAC patients harbor mutations in the oncogene KRAS, and these cells are dependent upon KRAS for survival.[4] Mutant-KRAS drives PDAC tumorigenesis and propagation[5] through a variety of mechanisms, including signaling for rewiring of metabolic pathways.[3–6] In particular, PDAC alters the metabolism of glutamine to facilitate cell proliferation.[6]

Glutamine is a major bioenergetic fuel for proliferating cells, as it generates nitrogen used for the biosynthesis of numerous essential molecules.[7] Canonically, glutamine is transported into the mitochondria and converted into glutamate by GLS1 (**Figure 1A**). Glutamate can be used for a

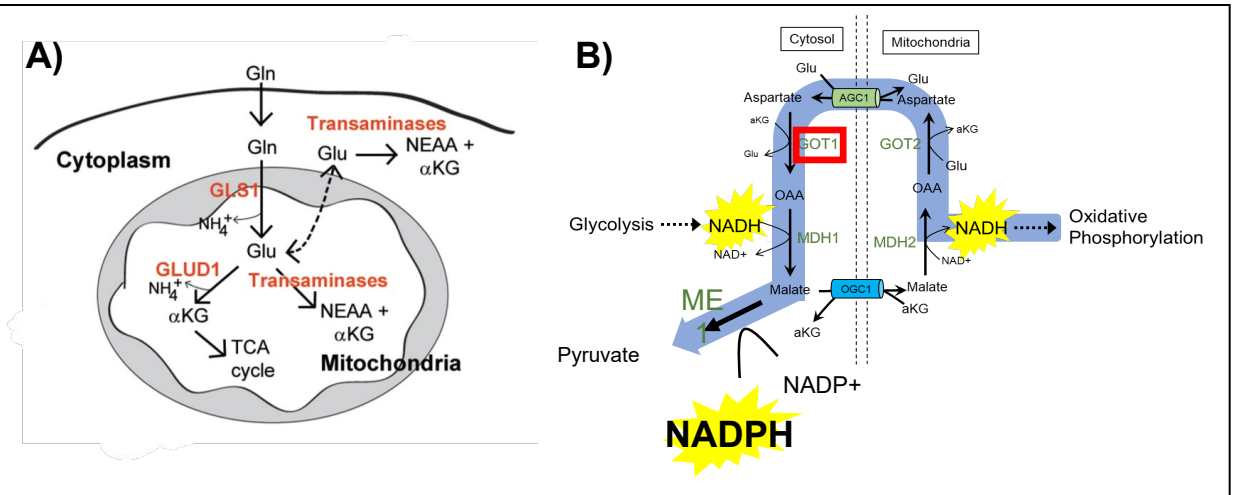

Figure 1. PDAC rewires glutamine metabolism. A) Canonical pathway of glutamine (Gln) metabolism. Figure from Son et al. *Nature* **2013**[6]. B) Non-canonical pathway of Gln metabolism in PDAC. The pathway proceeds through the malate-aspartate shuttle and is denoted in blue. GOT1 is highlighted in the red box. Figure adapted from Kremer et al. *Nat Comm* **2021**[8].

variety of cellular processes, including fueling the TCA cycle. GLUD1 converts glutamate to α-ketoglutarate (αKG), which enters the TCA cycle to generate energy for cellular functions and growth.[7] In PDAC, a non-canonical glutamine metabolic pathway is utilized to fuel cell growth (**Figure 1B**). Mutant-KRAS largely inactivates the GLUD1 pathway and instead promotes glutamine metabolism through the transaminase GOT1[6], which is part of the malate-aspartate shuttle. The shuttle facilitates the transport of electrons into the mitochondria to generate NADH for fueling oxidative phosphorylation. Previous work found that in PDAC, mitochondrial GOT2 is the primary source of αKG and aspartate, rather than GLUD1. Aspartate is transported to the cytosol, where GOT1 is responsible for converting it and αKG into oxaloacetate (OAA) and glutamate, respectively. OAA is reduced to malate by MDH1, then oxidized to pyruvate by ME1. The oxidation reaction by ME1 serves to generate NADPH, which is utilized to maintain cellular redox homeostasis and promote cellular proliferation.[6] GOT1 is dispensable in non-cancerous cells, whereas inhibition of GOT1 in PDAC stunts tumor growth and proliferation[8], indicating GOT1 is essential for PDAC survival.

Although GOT1 is known to facilitate exchange of an essential source of nitrogen flux via the non-canonical glutamine pathway in PDAC, little is known about which products this nitrogen is used to generate. Furthermore, how glutamine metabolism is rewired upon loss of GOT1 in surviving PDAC cells is also unknown. To interrogate how GOT1 knockdown affects glutamine metabolism in PDAC we used a multi-omic approach in which we utilized doxycycline inducible knockdown cells cultured in glutamine and performed RNA-sequencing and LC/MS metabolomics to study the genome and metabolome, respectively. After defining significant metabolic changes in steady state metabolomics, we examined transcriptomic changes, with a focus on metabolic transporters. Using this multi-omic approach we aimed to identify a nitrogen-driven metabolic signature upon GOT1 knockdown.

METHODS

RNA-Seq Analysis

RNA-Seq data for doxycycline-inducible shRNA knockdown of GOT1 in Tu8902 cells, a human pancreatic cancer cell line, was identified and accessed through the Gene Expression Omnibus (GEO) database[9,10] (project accession number: GSE157830[8]). Raw sequencing data (**Table 1**) was downloaded from the Sequence Read Archive (SRA)[11] (SRA study number: SRP282058[8]) using sratoolkit[12] (ver 2.10.9).

Table 1. Raw sequencing data SRA and GEO accession numbers, cell line of origin, and treatment.

SRA Run Accession	GEO Accession	Sample Cell Line	Treatment
SRR12624085	GSM4775595	Tu8902	Control
SRR12624086	GSM4775596	Tu8902	Control
SRR12624087	GSM4775597	Tu8902	Control
SRR12624088	GSM4775598	Tu8902	GOT1 knockdown
SRR12624089	GSM4775599	Tu8902	GOT1 knockdown
SRR12624090	GSM4775600	Tu8902	GOT1 knockdown

Adapter trimming, base correction, and quality pruning and filtering of sequenced reads was performed using fastp[13] (ver 0.23.4). fastp also provided assessment of data quality pre- and post-trimming and quality filtering. Reads were mapped, aligned, and counted using HISAT2[14] (ver 2.2.1). Lowly expressed genes (mean count of ≤ 1) were removed prior to differential expression analysis. Differential expression and visualization of results was performed with DESeq2[15] (ver 1.42.1), with correction of p-values using the Benjamini-Hochberg method.

Gene Set Enrichment Analysis

Genes with an FDR adjusted p-value < 0.05 and displaying a $|\log_2(\text{Fold Change})|$ of > 0.5 were retained as significant and differentially expressed for enrichment analysis. We chose the cutoff of $|\log_2(\text{Fold Change})|$ of > 0.5 to ensure we were capturing genes that may have subtle, but significant changes in expression. Selecting both directions for log FC allowed us to identify these differentially expressed genes in both upregulated and downregulated directions. Three sets of genes were then curated: one containing all differentially regulated genes, one with only differentially upregulated genes, and one with only differentially downregulated genes. Gene IDs of the differentially expressed genes were converted from Ensembl IDs to Entrez IDs in R[16] (ver 4.3.3) by R package AnnotationDbi[17] and org.Hs.eg.db[18] (ver 3.18.0). KEGG pathways were mapped to each of the datasets using R package clusterProfiler[19,20] (ver 4.10.0). Pathways were identified as enriched if they passed the adjusted p-value < 0.05 cutoff.

Metabolomics Sample Preparation

Tu8902 Doxycycline-inducible shRNA knockdown of GOT1 cells were cultured in DMEM with 10% FBS. Cells were cultured with 1 ng/mL of doxycycline for three days to induce GOT1 knockdown and verified by western blot. Knockdown cells and control cells were collected for metabolomics experiments with a liquid extraction consisting of quenching aspirated cells with 1mL of ice-cold 80% MeOH and 20% H_2O. Cells were scraped and incubated on dry ice for 10 minutes. Supernatant was collected and centrifuged for 10 minutes at 14,000 RPM. Samples were volume normalized by protein concentration, dried, and resuspended in 50 uL 50% MeOH and 50% H_2O.

Metabolomics Instrumentation

Samples were run on an Agilent 6545 Q-TOF coupled with an Agilent 1290 Infinity II liquid chromatography (LC) stack equipped with reverse-phase (RP) ion-pairing (IP) chromatography.

Samples were run in full-scan MS1 mode. Standards were included for a retention time (RT) library for compound identification. Data was collected in centroid mode.

Metabolomics Analysis

Data was processed with Agilent Masshunter Profinder (ver 10), using the targeted feature extraction via a metabolite reference library in Agilent PCDL (ver 7). Metabolites were verified with m/z and RT values and chromatogram peaks were manually inspected. Metabolite abundance was calculated by area under the curve (AUC). Raw data was exported in a CSV file.

Raw data was processed via MetaboAnalyst (ver 6.0) (freely available for online use at https://www.metaboanalyst.ca/MetaboAnalyst/)[21]. Data was input into the Statistical Analysis [one-factor] pipeline and normalized by median to account for systematic differences in instrument-loading for each sample. Data was scaled by Auto scaling, which is the mean-centered and divided by the standard deviation of each metabolite, then log 10 transformed. ANOVA was performed between the three groups (WT, sh1, sh3) with an alpha level of 0.05. Metabolite pathway enrichment analysis was performed via MetaboAnalyst with specification of KEGG pathways.

Integration of RNA-Seq and Metabolomic Data

Differentially expressed genes were integrated with metabolomic data using the joint pathway analysis tool provided by Metabolanalyst (ver 6.0)[21]. Differentially expressed genes with their associated Entrez IDs (from the gene set enrichment analysis) were categorized into up- and down-regulated groups and integrated with up- and down-regulated metabolomics data, respectively. Up- and down-regulated differentially expressed genes (Entrez IDs and $\log_2$(Fold Change) values) and metabolic data (KEGG compound IDs, from KEGG[22–24]) were uploaded to the Pathways module for Joint Pathway analysis. Data were tightly integrated (option: combined queries) and assessed for enrichment using the 'Metabolic Pathways' parameter. Enrichment

testing was performed using a Hypergeometric test. Topological analysis of pathway nodes was evaluated using the measure of degree centrality to generate the Pathway Impact Score, which describes the importance of up-/down-regulated genes/metabolites in the enriched pathways by considering the node numbers the regulated components link to in the network.

RESULTS

Transcriptomics analysis identifies candidate up- and down-regulated pathways

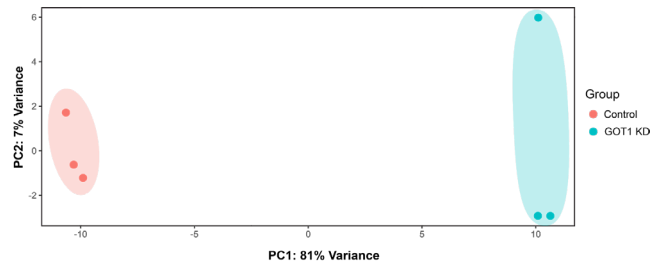

Figure 2. PCA plot of RNA-Seq samples. Samples clearly cluster by treatment group (control or GOT1 KD).

58,884 genes across the six samples were initially observed after alignment and counting. 21,626 remained after removal of lowly expressed genes. Comparison of samples by Principal Component Analysis (PCA) produced clustering based upon treatment (control versus GOT1 KD), with 81% of the variance in the data set attributed to the treatment (**Figure 2**).

Differentially expressed genes were identified via analysis with DESeq2, which uses empirical Bayesian modeling to estimate fold-change.[15] Of the 21,626 observed genes, 3464 genes displayed a $\log_2$(Fold Change) greater than 0.5 or less than -0.5 and an adjusted p-value < 0.05 (**Figure 3**). Importantly, GOT1 is a top significantly downregulated gene, as is expected upon GOT1 KD.

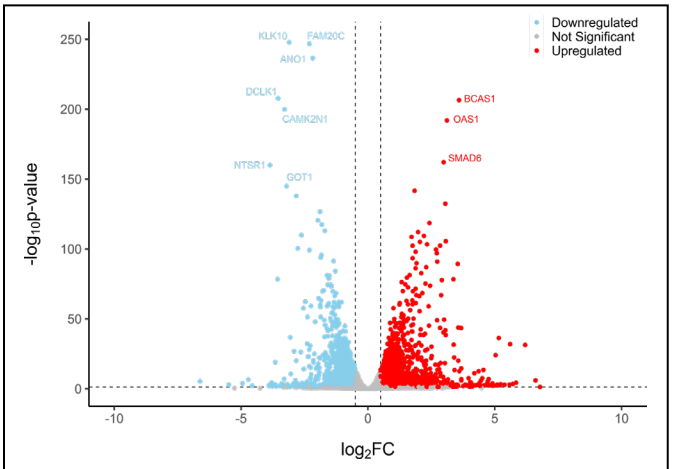

Figure 3. GOT1 KD differentially regulates thousands of genes. The significance threshold was set at an adjusted p-value < 0.05. Genes meeting the significance threshold with a $\log_2$(Fold Change) greater than 0.5 are denoted in red; those that are less than 0.5 are blue. Non-differentially expressed genes are gray. The top 10 differentially expressed genes are labeled.

We then performed gene set enrichment analysis using KEGG identifiers to determine the top 20 pathways across all upregulated and downregulated genes (**Figure 4A**). Top identified pathways include: efferocytosis, axon guidance, sphingolipid metabolism, and the C-type lectin receptor signaling pathway, among others, suggesting knockdown of GOT1 may impact more than just metabolic processes.

We wanted to know specifically which pathways were up- or down-regulated upon GOT1 KD. After partitioning the differentially expressed genes by up- or downregulation, we repeated the KEGG-based gene set enrichment analysis to determine which pathways were differentially regulated. For upregulated genes, four pathways were identified: efferocytosis (the clearance of apoptotic cells by phagocytes), lysosome, axon guidance, and β-alanine metabolism (**Figure 4B**), indicating that GOT1 KD upregulates not only a metabolic pathway, but potentially signaling pathways related to cell death.

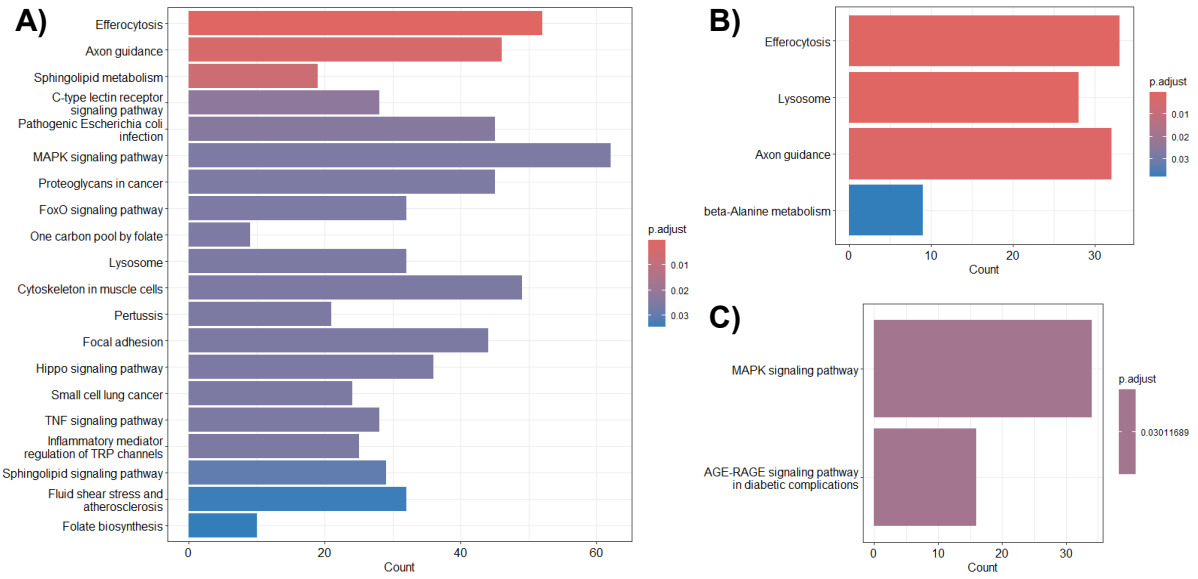

Figure 4. KEGG annotated pathways enriched upon GOT1 knockdown. A) KEGG annotated pathways identified for all genes identified as significantly differentially expressed in GOT1 KD Tu8902 cells. **B)** KEGG annotated pathways for significantly upregulated genes in GOT1 KD Tu8902 cells. **C)** KEGG annotated pathways for significantly downregulated genes in GOT1 KD Tu8902 cells.

Downregulated genes only had two identified processes/associations: MAPK signaling pathway and AGE-RAGE signaling pathway in diabetic complications (**Figure 4C**). These results imply

GOT1 KD does not impair metabolic processes, but instead promotes downregulation of the RAGE and MAPK signaling pathways. These intertwined signaling pathways are responsible for directing numerous cellular processes, including proliferation[25,26], thus suggesting possible inhibition of PDAC proliferation.

GOT1 knockdown alters nucleotide pools

To build upon the findings from the genome, the metabolome was studied by knocking down GOT1 in Tu8902 cells via doxycycline incubation for 3 days and running on an LC/MS platform. Samples consisted of 6 replicate groups (sh-NT +/- dox, sh1 +/- dox, sh3 +/-dox) with 3 phenotypic analysis groups (WT, sh1, sh3). Given that the knockdown of GOT1 is induced by the addition of doxycycline, all groups that were minus dox, regardless of hairpin status were assigned to the WT group, as well as the sh-NT plus dox group. This resulted in 12 samples in the WT control group, and 3 samples each in the sh1 and sh3 GOT1 knockdown groups. The three groups separated on the PCA plot and clustered via unsupervised clustering in the sample dendrogram **(Figure 5)**.

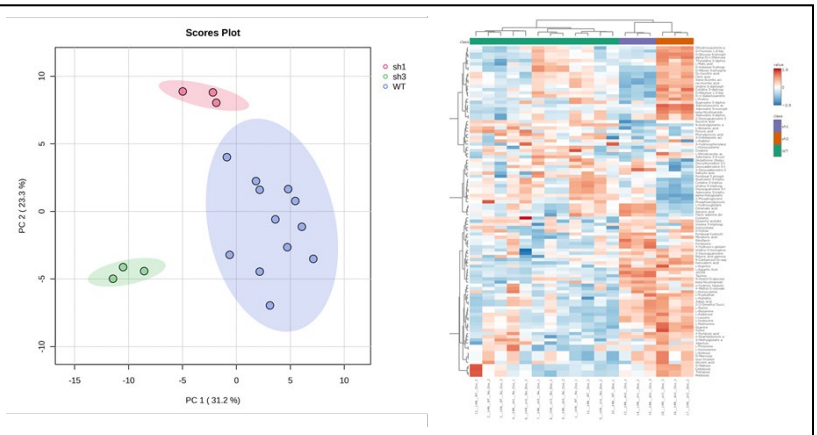

Figure 5. GOT1 knockdown shows distinct metabolic profiles. Left: PCA plot for WT, sh1, and sh3 sample groups. PC1 and PC2 are plotted. Right: Heatmap for normalized metabolite abundance profiles. Unsupervised hierarchical clustering on rows (metabolites) and columns (samples).

ANOVA was performed at an alpha level of 0.05, producing 60 significantly altered metabolites upon GOT1 knockdown. Given that the RNA-seq experiments were performed on the sh3 knockdown cells, further analysis focused on the same paired samples for metabolomics. In this subset there were 12 significantly decreased metabolites in the GOT1 KD group largely consisting

Metabolite	KEGG ID
Oxoglutaric acid	C00026
2-Phosphoglyceric acid	C00631
Guanosine triphosphate	C00044
Adenosine triphosphate	C00002
dGTP	C00286
Uridine triphosphate	C00075
Cytidine triphosphate	C00063
Phosphoenolpyruvic acid	C00074
dTDP	C00363
N-Acetyl-L-glutamic acid	C00624
Deoxyadenosine triphosphate	C00131
dADP	C00206

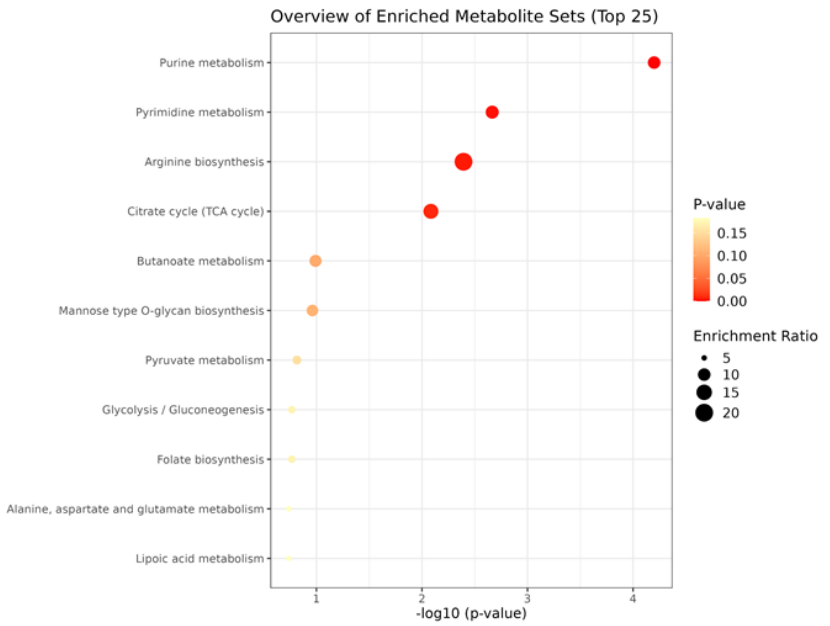

Figure 6. Significantly decreased metabolites upon GOT1 knockdown. Left: Metabolites significantly decreased upon GOT1 knockdown in sh3 group. $p < 0.05$. Right: Pathway enrichment analysis for significantly decreased metabolites (shown left) via KEGG pathways.

of triphosphate nucleotides **(Figure 6)**. There were 36 significantly increased metabolites in the knockdown group across a wider array of metabolic pathways. Enriched pathways included alanine, aspartate, and glutamate metabolism, as well as mono and diphosphate nucleotides

Metabolite	KEGG ID	Metabolite	KEGG ID
Taurine	C00245	Fructose 1,6-bisphosphate	C00354
cis-Aconitic acid	C00417	Proline	C00148
trans-Aconitic acid	C02341	Serine	C00065
AICAR	C04677	Glutamine	C00064
Citric acid	C00158	CDP	C00112
(1R,2R)-Isocitric acid	C04617	Ureidosuccinic acid	C00438
Ribose 1,5-bisphosphate	C01151	Dihydroxyacetone phosphate	C00111
D-Galactosamine	C02262	L-Tryptophan	C00078
Methylsuccinic acid	C08645	L-Aspartic acid	C00049
Adipic acid	C06104	D-Xylitol	C00379
4-Guanidinobutanoic acid	C01035	2-Oxovaleric acid	C06255
4-Pyridoxic acid	C00847	beta-Nicotinamide mononucleotide	C00455
Isoleucine	C00407	Methionine	C00073
Leucine	C00123	D-Mannose 1-phosphate	C00636
N-Acetyl-D-Glucosamine 6-Phosphate	C00357	Glucose 6-phosphate	C00092
Uridine 5'-diphosphate	C00015	Guanine	C00242
L-Arginine	C00062	Adenosine monophosphate	C00020
L-Arabinose	C00259	Adenylsuccinic acid	C03794

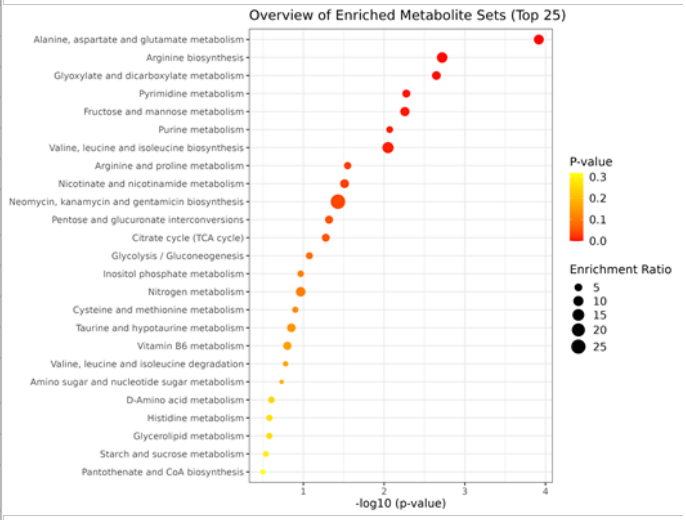

Figure 7. Significantly increased metabolites upon GOT1 knockdown. Left: Metabolites significantly increased upon GOT1 knockdown in sh3 group. $p < 0.05$. Right: Pathway enrichment analysis for significantly increased metabolites (shown left) via KEGG pathways.

(**Figure 7**). These results indicate that the loss of GOT1 may influence triphosphate nucleotide pools and thus accumulate lowly phosphate nucleotides.

Integrating transcriptomics and metabolomics data reveals the interference of a large range of pathways by GOT1 knockdown

Using Metaboanalyst, we integrated our metabolite and transcriptomic data by performing joint enrichment with respect to KEGG pathways. Up- and down-regulated genes/metabolites were enriched, respectively. The upregulated genes and metabolites were strongly significantly enriched in four metabolic pathways, including sphingolipid metabolism, glycerolipid metabolism, β-alanine metabolism, and mucin type O-glycan biosynthesis (**Figure 8A**). A further six enriched pathways passed the 0.05 raw p-value cut-off. These ten pathways are predominantly comprised of nitrogen compound-associated metabolic processes, including the metabolism of several amino acids and lipids.

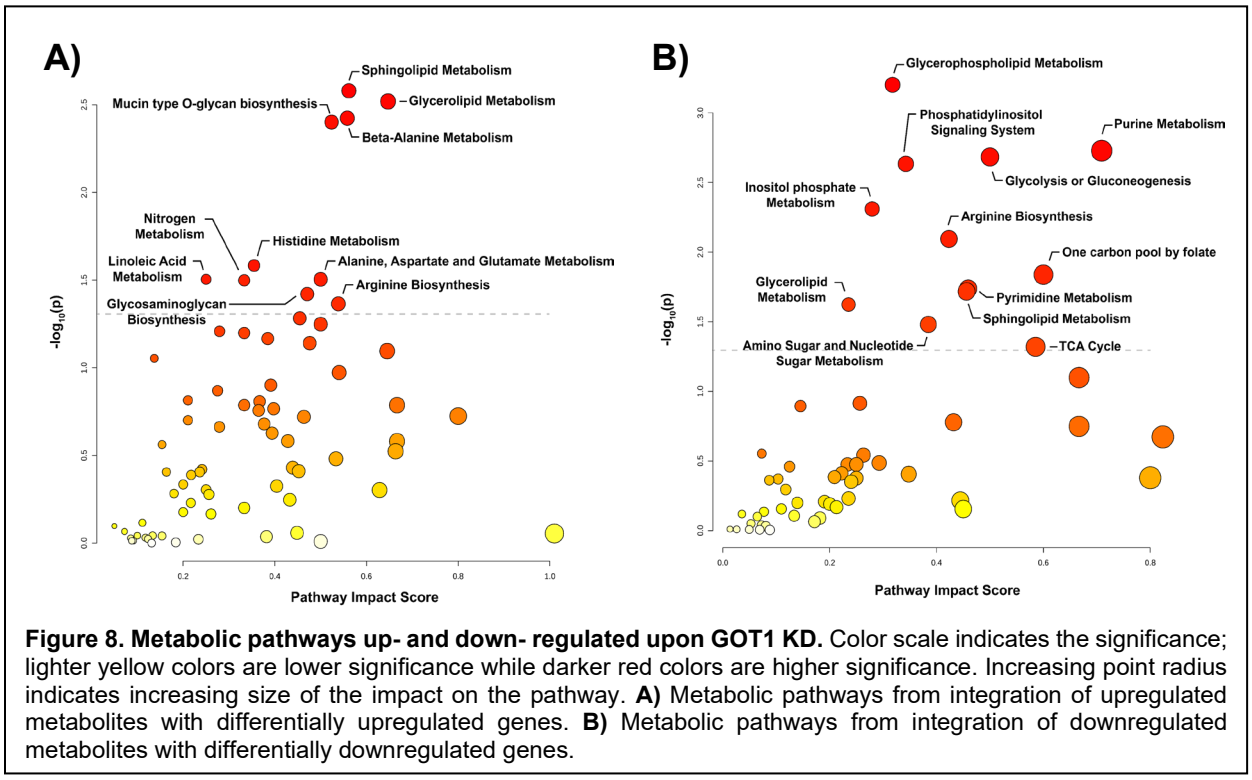

Figure 8. Metabolic pathways up- and down- regulated upon GOT1 KD. Color scale indicates the significance; lighter yellow colors are lower significance while darker red colors are higher significance. Increasing point radius indicates increasing size of the impact on the pathway. **A)** Metabolic pathways from integration of upregulated metabolites with differentially upregulated genes. **B)** Metabolic pathways from integration of downregulated metabolites with differentially downregulated genes.

The down-regulated genes and metabolites were enriched into 12 metabolic pathways with raw p-values less than 0.05 (**Figure 8B**). In addition to nitrogen compound-associated and lipid metabolisms, several carbohydrate metabolic processes were found in this enrichment. Purine and pyrimidine metabolism were down-regulated upon GOT1 knockdown, matching the decrease in adenosine, guanosine, cytidine, thymine, and uridine levels in our targeted metabolomic data (**Figure 6**) Therefore, the knockdown of GOT1 may restrict purine and pyrimidine biosynthesis in PDAC cells. Notably, some pathways showed up in both enrichment results, such as sphingolipid metabolism, glycerolipid metabolism, and arginine biosynthesis, indicating both up- and down-regulated components in these pathways under GOT1 knockdown. For example, some components in the urea cycle of arginine biosynthesis were upregulated, while the levels of some genes and metabolites related to glutamates in arginine biosynthesis decreased. The pathway impact scores, which show how important the regulated components are in the pathway, ranged widely between 0.2 and 0.7 in both up- and down-regulated enriched pathways.

DISCUSSION

Knockdown of GOT1 in PDAC displays a clear nitrogen-driven metabolic signature. As PDAC relies upon GOT1 for production of OAA and glutamate, loss of GOT1 upon knockdown would affect glutamate, and ultimately glutamine, production. A reduction in cellular glutamine levels would affect purine and pyrimidine metabolism, and amino sugar and nucleotide sugar metabolism, among others[24]. Our integrated transcriptomic and metabolomic data revealed down-regulation of these (and other nitrogen-containing compound) pathways. Of note is a restriction in purine and pyrimidine metabolism. Impaired purine and pyrimidine metabolism suggests that DNA and/or RNA synthesis, and thus cell proliferation, are likely inhibited. While previous work shows that GOT1 knockdown does inhibit proliferation and stunts tumor growth[8], further studies are needed to confirm whether DNA and/or RNA synthesis is actively diminished.

Interestingly, we noticed that certain metabolic pathways were noted as both up- and down-regulated. We chose to focus further on sphingolipid metabolism, as the signaling molecules sphingosine-1-phosphate (S1P) and ceramide-1-phosphate (C1P) (both of which contain nitrogen) are known to be involved in general cancer progression[27], as well as in PDAC[28–32]. Closer inspection of our dual pathway results revealed the downregulation of an enzyme promoting the creation of S1P (SPHK1) and upregulation of an enzyme (PLPP3) reverting S1P and C1P to sphingosine and ceramide, respectively. S1P is a signaling molecule involved in numerous cellular processes, including regulation of epigenetics and transcription[27], cell survival, migration, proliferation, and immune cell recruitment[28]. In PDAC, S1P metabolism is thought to be dysregulated[29], as S1P levels are significantly higher than surrounding non-cancerous cells, and the activity of SPHK1/2 to produce S1P results in cellular proliferation, migration, and drug resistance[28]. Akin to S1P, C1P also promotes cell growth, survival, and migration[31,32]. PDAC cells were shown to release extracellular vesicles containing C1P, which recruits pancreatic cancer stem cells to maintain tumor growth[31].

If knockdown of GOT1 truly upregulates PLPP3 and downregulates SPHK1 expression, this implies defects should be noted in proliferation, survival, and migration, as well as a reduction in C1P and S1P levels. PDAC proliferation is noted to be stunted upon GOT1 knockdown[8], but not upon SPHK1 knockout (SPHK1 knockout resulted in increased sensitivity to chemotherapies)[28]. Little is known regarding how PLPP3 affects PDAC progression, so future work could focus on elucidating the mechanisms by which PLPP3 may contribute to PDAC. Further, C1P and S1P levels were not differentially regulated (either up or down), implying little, if any, significant impact on sphingolipid metabolism. Work is needed to elucidate if the up- and down-regulation of enzymatic members of the sphingolipid metabolism pathway upon GOT1 knockdown can contribute to cell survival, migration, and proliferation in a sphingolipid-independent manner or if they may cause more subtle changes in nitrogen-based metabolic flux and signaling.

Using untargeted metabolomics analysis in the future may help us capture the complex regulations in these pathways, as it can identify a larger variety of metabolites – including intermediate metabolites – than the targeted metabolomics we used in this study. Although there are many details that need to be clarified, the involvement of sphingolipid metabolism and other signaling molecule metabolisms (e.g. phosphatidylinositol signaling) upon GOT1 knockdown showed a potential linkage from energy metabolism to intercellular signals that play roles in PDAC microenvironment construction and metastasis.

ACKNOWLEDGMENTS

We thank Peter Sajjakulnukit and the Costas Lyssiotis lab for providing the metabolomic data. Thank you to Chase Weidmann, Ph.D. for his help in troubleshooting errors in quality control, trimming, and mapping of transcriptomic data. Finally, we thank the course directors, Alex Tsoi, Ph.D. and Steven Parker, Ph.D. for their instruction and insightful comments on our proposal, and the course graduate student instructors, Cynthia Zajac and Jingxian Zhao, for their assistance throughout the process.

PROJECT CONTRIBUTIONS

K.H. retrieved, quality checked and filtered, trimmed, and mapped transcriptomic data. M.A. performed differential expression analysis on transcriptomic data. Z.T. identified enriched KEGG pathways in transcriptomic data. P.S. processed and analyzed all metabolomic data. T.M. identified differentially regulated metabolic pathways from integrated transcriptomic and metabolomic data. All members contributed to the generation of figures and the writing and editing of this manuscript.

REFERENCES

(1) Siegel, R. L.; Miller, K. D.; Wagle, N. S.; Jemal, A. Cancer Statistics, 2023. *CA. Cancer J. Clin.* **2023**, *73* (1), 17–48. https://doi.org/10.3322/caac.21763.

(2) *Abeloff's Clinical Oncology*, Fifth edition.; Niederhuber, J. E., Armitage, J. O., Doroshow, J. H., Kastan, M. B., Tepper, J. E., Eds.; Elsevier Churchill Livingstone: Philadelphia, Pennsylvania, 2014.

(3) Halbrook, C. J.; Lyssiotis, C. A. Employing Metabolism to Improve the Diagnosis and Treatment of Pancreatic Cancer. *Cancer Cell* **2017**, *31* (1), 5–19. https://doi.org/10.1016/j.ccell.2016.12.006.

(4) Ying, H.; Kimmelman, A. C.; Lyssiotis, C. A.; Hua, S.; Chu, G. C.; Fletcher-Sananikone, E.; Locasale, J. W.; Son, J.; Zhang, H.; Coloff, J. L.; Yan, H.; Wang, W.; Chen, S.; Viale, A.; Zheng, H.; Paik, J.; Lim, C.; Guimaraes, A. R.; Martin, E. S.; Chang, J.; Hezel, A. F.; Perry, S. R.; Hu, J.; Gan, B.; Xiao, Y.; Asara, J. M.; Weissleder, R.; Wang, Y. A.; Chin, L.; Cantley, L. C.; DePinho, R. A. Oncogenic Kras Maintains Pancreatic Tumors through Regulation of Anabolic Glucose Metabolism. *Cell* **2012**, *149* (3), 656–670. https://doi.org/10.1016/j.cell.2012.01.058.

(5) Perera, R. M.; Bardeesy, N. Pancreatic Cancer Metabolism: Breaking It Down to Build It Back Up. *Cancer Discov.* **2015**, *5* (12), 1247–1261. https://doi.org/10.1158/2159-8290.CD-15-0671.

(6) Son, J.; Lyssiotis, C. A.; Ying, H.; Wang, X.; Hua, S.; Ligorio, M.; Perera, R. M.; Ferrone, C. R.; Mullarky, E.; Shyh-Chang, N.; Kang, Y.; Fleming, J. B.; Bardeesy, N.; Asara, J. M.; Haigis, M. C.; DePinho, R. A.; Cantley, L. C.; Kimmelman, A. C. Glutamine Supports Pancreatic Cancer Growth through a KRAS-Regulated Metabolic Pathway. *Nature* **2013**, *496* (7443), 101–105. https://doi.org/10.1038/nature12040.

(7) DeBerardinis, R. J.; Cheng, T. Q's next: The Diverse Functions of Glutamine in Metabolism, Cell Biology and Cancer. *Oncogene* **2010**, *29* (3), 313–324.

https://doi.org/10.1038/onc.2009.358.

(8) Kremer, D. M.; Nelson, B. S.; Lin, L.; Yarosz, E. L.; Halbrook, C. J.; Kerk, S. A.; Sajjakulnukit, P.; Myers, A.; Thurston, G.; Hou, S. W.; Carpenter, E. S.; Andren, A. C.; Nwosu, Z. C.; Cusmano, N.; Wisner, S.; Mbah, N. E.; Shan, M.; Das, N. K.; Magnuson, B.; Little, A. C.; Savani, M. R.; Ramos, J.; Gao, T.; Sastra, S. A.; Palermo, C. F.; Badgley, M. A.; Zhang, L.; Asara, J. M.; McBrayer, S. K.; di Magliano, M. P.; Crawford, H. C.; Shah, Y. M.; Olive, K. P.; Lyssiotis, C. A. GOT1 Inhibition Promotes Pancreatic Cancer Cell Death by Ferroptosis. *Nat. Commun.* **2021**, *12* (1), 4860. https://doi.org/10.1038/s41467-021-24859-2.

(9) Edgar, R. Gene Expression Omnibus: NCBI Gene Expression and Hybridization Array Data Repository. *Nucleic Acids Res.* **2002**, *30* (1), 207–210. https://doi.org/10.1093/nar/30.1.207.

(10) Barrett, T.; Wilhite, S. E.; Ledoux, P.; Evangelista, C.; Kim, I. F.; Tomashevsky, M.; Marshall, K. A.; Phillippy, K. H.; Sherman, P. M.; Holko, M.; Yefanov, A.; Lee, H.; Zhang, N.; Robertson, C. L.; Serova, N.; Davis, S.; Soboleva, A. NCBI GEO: Archive for Functional Genomics Data Sets—Update. *Nucleic Acids Res.* **2012**, *41* (D1), D991–D995. https://doi.org/10.1093/nar/gks1193.

(11) Leinonen, R.; Sugawara, H.; Shumway, M.; on behalf of the International Nucleotide Sequence Database Collaboration. The Sequence Read Archive. *Nucleic Acids Res.* **2011**, *39* (Database), D19–D21. https://doi.org/10.1093/nar/gkq1019.

(12) NCBI SRA Team. SRA Tools. https://github.com/ncbi/sra-tools (accessed 2024-04-09).

(13) Chen, S.; Zhou, Y.; Chen, Y.; Gu, J. Fastp: An Ultra-Fast All-in-One FASTQ Preprocessor. *Bioinformatics* **2018**, *34* (17), i884–i890. https://doi.org/10.1093/bioinformatics/bty560.

(14) Kim, D.; Paggi, J. M.; Park, C.; Bennett, C.; Salzberg, S. L. Graph-Based Genome Alignment and Genotyping with HISAT2 and HISAT-Genotype. *Nat. Biotechnol.* **2019**, *37* (8), 907–915. https://doi.org/10.1038/s41587-019-0201-4.

(15) Love, M. I.; Huber, W.; Anders, S. Moderated Estimation of Fold Change and Dispersion for RNA-Seq Data with DESeq2. *Genome Biol.* **2014**, *15* (12), 550.

https://doi.org/10.1186/s13059-014-0550-8.

(16) R Core Team. R: A Language and Environment for Statistical Computing, 2024. https://www.R-project.org/.

(17) Pagès, H.; Carlson, M.; Falcon, S.; Li, N. AnnotationDbi: Manipulation of SQLite-Based Annotations in Bioconductor, 2023. https://doi.org/10.18129/B9.BIOC.ANNOTATIONDBI.

(18) Carlson, M. Org.Hs.Eg.Db: Genome Wide Annotation for Human, 2023. DOI: 10.18129/B9.bioc.org.Hs.eg.db.

(19) Yu, G.; Wang, L.-G.; Han, Y.; He, Q.-Y. ClusterProfiler: An R Package for Comparing Biological Themes Among Gene Clusters. *OMICS J. Integr. Biol.* **2012**, *16* (5), 284–287. https://doi.org/10.1089/omi.2011.0118.

(20) Wu, T.; Hu, E.; Xu, S.; Chen, M.; Guo, P.; Dai, Z.; Feng, T.; Zhou, L.; Tang, W.; Zhan, L.; Fu, X.; Liu, S.; Bo, X.; Yu, G. ClusterProfiler 4.0: A Universal Enrichment Tool for Interpreting Omics Data. *The Innovation* **2021**, *2* (3), 100141. https://doi.org/10.1016/j.xinn.2021.100141.

(21) Ewald, J. D.; Zhou, G.; Lu, Y.; Kolic, J.; Ellis, C.; Johnson, J. D.; Macdonald, P. E.; Xia, J. Web-Based Multi-Omics Integration Using the Analyst Software Suite. *Nat. Protoc.* **2024**. https://doi.org/10.1038/s41596-023-00950-4.

(22) Kanehisa, M. KEGG: Kyoto Encyclopedia of Genes and Genomes. *Nucleic Acids Res.* **2000**, *28* (1), 27–30. https://doi.org/10.1093/nar/28.1.27.

(23) Kanehisa, M. Toward Understanding the Origin and Evolution of Cellular Organisms. *Protein Sci.* **2019**, *28* (11), 1947–1951. https://doi.org/10.1002/pro.3715.

(24) Kanehisa, M.; Furumichi, M.; Sato, Y.; Kawashima, M.; Ishiguro-Watanabe, M. KEGG for Taxonomy-Based Analysis of Pathways and Genomes. *Nucleic Acids Res.* **2023**, *51* (D1), D587–D592. https://doi.org/10.1093/nar/gkac963.

(25) Linehan, A.; O'Reilly, M.; McDermott, R.; O'Kane, G. M. Targeting KRAS Mutations in Pancreatic Cancer: Opportunities for Future Strategies. *Front. Med.* **2024**, *11*, 1369136. https://doi.org/10.3389/fmed.2024.1369136.

(26) Swami, P.; Thiyagarajan, S.; Vidger, A.; Indurthi, V. S. K.; Vetter, S. W.; Leclerc, E. RAGE Up-Regulation Differently Affects Cell Proliferation and Migration in Pancreatic Cancer Cells. *Int. J. Mol. Sci.* **2020**, *21* (20), 7723. https://doi.org/10.3390/ijms21207723.

(27) Wang, P.; Yuan, Y.; Lin, W.; Zhong, H.; Xu, K.; Qi, X. Roles of Sphingosine-1-Phosphate Signaling in Cancer. *Cancer Cell Int.* **2019**, *19* (1), 295. https://doi.org/10.1186/s12935-019-1014-8.

(28) Yuza, K.; Nakajima, M.; Nagahashi, M.; Tsuchida, J.; Hirose, Y.; Miura, K.; Tajima, Y.; Abe, M.; Sakimura, K.; Takabe, K.; Wakai, T. Different Roles of Sphingosine Kinase 1 and 2 in Pancreatic Cancer Progression. *J. Surg. Res.* **2018**, *232*, 186–194. https://doi.org/10.1016/j.jss.2018.06.019.

(29) Gao, Z.; Janakiraman, H.; Xiao, Y.; Kang, S. W.; Dong, J.; Choi, J.; Ogretmen, B.; Lee, H.-S.; Camp, E. R. Sphingosine-1-Phosphate Inhibition Increases Endoplasmic Reticulum Stress to Enhance Oxaliplatin Sensitivity in Pancreatic Cancer. *World J. Oncol.* **2024**, *15* (2), 169–180. https://doi.org/10.14740/wjon1768.

(30) Kuc, N.; Doermann, A.; Shirey, C.; Lee, D. D.; Lowe, C.-W.; Awasthi, N.; Schwarz, R. E.; Stahelin, R. V.; Schwarz, M. A. Pancreatic Ductal Adenocarcinoma Cell Secreted Extracellular Vesicles Containing Ceramide-1-Phosphate Promote Pancreatic Cancer Stem Cell Motility. *Biochem. Pharmacol.* **2018**, *156*, 458–466. https://doi.org/10.1016/j.bcp.2018.09.017.

(31) Presa, N.; Gomez-Larrauri, A.; Rivera, I.-G.; Ordoñez, M.; Trueba, M.; Gomez-Muñoz, A. Regulation of Cell Migration and Inflammation by Ceramide 1-Phosphate. *Biochim. Biophys. Acta BBA - Mol. Cell Biol. Lipids* **2016**, *1861* (5), 402–409. https://doi.org/10.1016/j.bbalip.2016.02.007.

(32) Rivera, I.-G.; Ordoñez, M.; Presa, N.; Gangoiti, P.; Gomez-Larrauri, A.; Trueba, M.; Fox, T.; Kester, M.; Gomez-Muñoz, A. Ceramide 1-Phosphate Regulates Cell Migration and Invasion of Human Pancreatic Cancer Cells. *Biochem. Pharmacol.* **2016**, *102*, 107–119.

https://doi.org/10.1016/j.bcp.2015.12.009.